Mechanisms of Ageing and Development 201 (2022) 111617

Contents lists available at ScienceDirect

Mechanisms of Ageing and Development

journal homepage: www.elsevier.com/locate/mechagedev

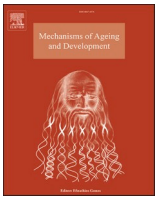

α-1 Adrenergic receptor antagonist doxazosin reverses hepatic stellate cells activation *via* induction of senescence

Sandra A. Serna-Salas [a,b], Johanna C. Arroyave-Ospina [b], Mengfan Zhang [b], Turtushikh Damba [b,e], Manon Buist-Homan [b,c], Martin H. Muñoz-Ortega [d], Javier Ventura-Juárez [a,*], Han Moshage [b,c]

[a] Dept. Morphology, Autonomous University of Aguascalientes, Aguascalientes, Mexico
[b] Dept. Gastroenterology and Hepatology, University of Groningen, University Medical Center Groningen, Groningen, the Netherlands
[c] Dept. Laboratory Medicine, University of Groningen, University Medical Center Groningen, Groningen, the Netherlands
[d] Dept. Chemistry, Autonomous University of Aguascalientes, Aguascalientes, Mexico
[e] School of Pharmacy, Mongolian National University of Medical Sciences, Ulaanbaatar, Mongolia

ARTICLE INFO

Keywords:
Stellate cells
Liver fibrosis
Senescence
α1-Adrenergic signaling
Norepinephrine
Protein kinase C
Phospholipase C
Cell proliferation

ABSTRACT

Background: Activated hepatic stellate cells (aHSCs) are the main effector cells during liver fibrogenesis. α-1 adrenergic antagonist doxazosin (DX) was shown to be anti-fibrotic in an *in vivo* model of liver fibrosis (LF), but the mechanism remains to be elucidated. Recent studies suggest that reversion of LF can be achieved by inducing cellular senescence characterized by irreversible cell-cycle arrest and acquisition of the senescence-associated secretory phenotype (SASP).
Aim: To elucidate the mechanism of the anti-fibrotic effect of DX and determine whether it induces senescence.
Methods: Primary culture-activated rat HSCs were used. mRNA and protein expression were measured by qPCR and Western blot, respectively. Cell proliferation was assessed by BrdU incorporation and xCelligence analysis. TGF-β was used for maximal HSC activation. Norepinephrine (NE), PMA and m-3M3FBS were used to activate alpha-1 adrenergic signaling.
Results: Expression of *Col1α1* was significantly decreased by DX (10 μmol/L) at mRNA (−30 %) and protein level (−50 %) in TGF-β treated aHSCs. DX significantly reduced aHSCs proliferation and increased expression of senescence and SASP markers. PMA and m-3M3FBS reversed the effect of DX on senescence markers.
Conclusion: Doxazosin reverses the fibrogenic phenotype of aHSCs and induces the senescence phenotype.

1. Introduction

Liver fibrosis is the excessive deposition of collagen type 1 in the extracellular matrix (ECM) as a result of an uncontrolled wound-healing response caused by chronic liver inflammation. Activated hepatic stellate cells (aHSCs) are the major source of excessive ECM production. During chronic liver injury, hepatic stellate cells undergo an activation process and transdifferentiate into myofibroblast-like cells, accompanied by several phenotypic changes, such as *de novo* expression of alpha-smooth muscle actin (αSMA), increased proliferation, loss of retinoid-storing capacity and the acquisition of fibrogenic functions (Rippe and Brenner, 2004). Therefore, the suppression of stellate cell activation is a valid strategy to treat hepatic fibrosis and/or cirrhosis. It has been described that senescence, a state of irreversible cell cycle arrest, may (partially) reverse stellate cell activation. Senescence is a process that permanently suppresses cell proliferation (Krizhanovsky et al., 2008). Senescent cells exhibit metabolic reprogramming, including the acquisition of the so-called *Senescence-Associated Secretory Phenotype* (SASP) (Coppé et al., 2010a,b), characterized by increased expression of cytokines like interleukin-6 (IL-6) and proteases like matrix metalloproteinase 9 (MMP-9) (Aoshiba et al., 2013; Schnabl et al., 2003). Senescent cells also have increased activity of β-galactosidase (SA-β-gal) (Dimri et al., 1995).

Senescence is regulated by the p53/p21 and p16INK4a/Rb pathways (Narita et al., 2003). Studies demonstrated that senescence induction in aHSCs reduces gene expression of collagen type 1 and fibronectin but not αSMA and GFAP (Krizhanovsky et al., 2008; Schnabl et al., 2003), suggesting that aHSCs maintain their morphology but (partially) reduce

* Corresponding author.
E-mail address: jventur@correo.uaa.mx (J. Ventura-Juárez).

https://doi.org/10.1016/j.mad.2021.111617
Received 10 August 2021; Received in revised form 6 December 2021; Accepted 21 December 2021
Available online 24 December 2021

their fibrogenic function.

Adrenergic receptors (AR) are a family of G protein-coupled receptors (Strosberg, 1993) and control several intracellular functions (cell proliferation and metabolic functions) (Han et al., 2008; García-Sáinz et al., 1999). Alpha-1 AR is coupled to the Gq protein, which induces the activation of phospholipase C (PLC) and protein kinase C (PKC), and the release of calcium (Ca^{2+}) from the endoplasmic reticulum (ER). The ligands of AR are norepinephrine (NE) and epinephrine (8). In HSCs, NE increases the proliferation of aHSCs (Oben et al., 2003; Sigala et al., 2013) and stimulates collagen gene expression *via* α1-AR (Oben et al., 2003). We previously showed that doxazosin has anti-fibrotic properties and reduces the expression of fibrotic markers (TGF-β, TIMP-2 and type 1 collagen *in vivo*) (Serna-Salas et al., 2018). Since these experiments were performed *in vivo*, the target cell of doxazosin could be not determined, and the effect of DX might be an indirect or direct effect on aHSCs *via* antagonism of the α1-AR. Furthermore, it is not known whether antagonism of the α1-AR by doxazosin modulates senescence of aHSCs. The aim of this study was to elucidate the mechanism of the anti-fibrotic effect of doxazosin on aHSCs and to determine whether doxazosin induces senescence in aHSCs.

2. Materials and methods

2.1. Animals

All animal care complied with the legal requirements approved by the guidelines of Institutional Animal Care and Use Committee of Laboratory Animals of the University of Groningen (DEC-RUG). Experimental procedures were approved by the appropriate Animal ethics Committee. All experiments were performed in accordance with relevant guidelines and regulations.

2.2. Cell isolation and culture

HSCs were isolated from male Wistar rats (300 g; Charles River Laboratories Inc., Wilmington, MA, USA) by Pronase-E (Merck, Amsterdam, the Netherlands) and collagenase (Roche, Almere, the Netherlands) perfusion and Nycodenz (13 %) (Axis-Shield POC, Oslo, Norway) gradient centrifugation as described previously (Damba et al., 2019). HSCs were cultured in a humidified atmosphere of 5% CO_2 at 37 °C in Iscove's Modified Dulbecco's Medium (IMDM) with Glutamax (Thermo Fisher Scientific, Waltham, MA, USA), supplemented with 20 % heat-inactivated fetal calf serum (Thermo Fisher Scientific), 1% sodium pyruvate (Thermo Fisher Scientific), 1% MEM non-essential amino acids (Thermo Fisher Scientific), 0.1 % gentamycin (Thermo Fisher Scientific), 100 U/mL penicillin (Lonza, Vervier, Belgium), 10 µg/mL streptomycin (Lonza) and 250 ng/mL fungizone (Lonza). Primary HSCs undergo spontaneous activation upon 7 days of culture on tissue culture plastic, showing increased proliferation, collagen synthesis and loss of retinoids. For studies on quiescent HSCs (qHSCs), cells were cultured in 6-well plates and treated one day after their isolation, for aHSCs, cells were cultured for 7 days on tissue culture plastic to obtain complete

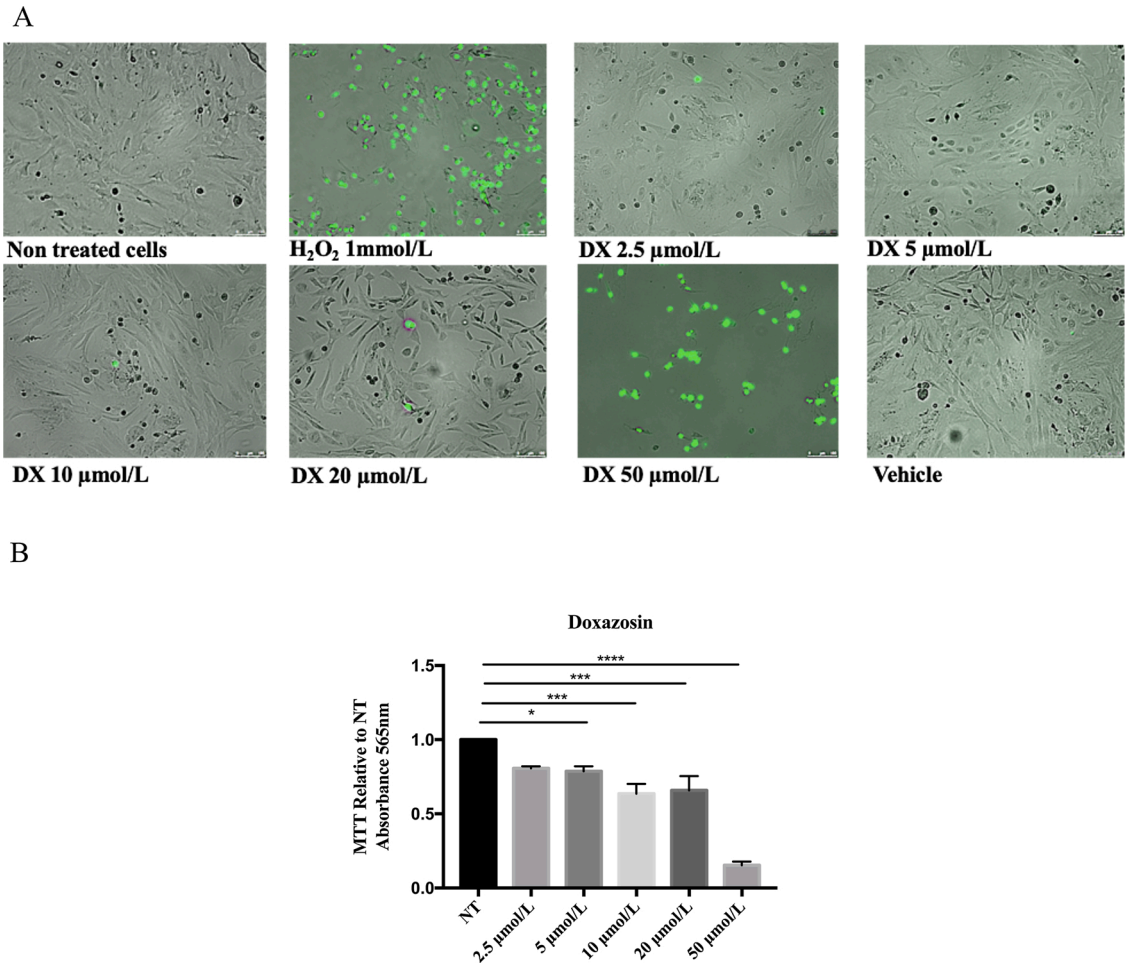

Fig. 1. DX toxicity towards aHSCs. A: Doxazosin did not induce toxicity in aHSC in the range of 2.5-20 µmol/L; scale bar 100 µm. **B:** MMT assay showed that DX concentrations of 50 µmol/L and higher significantly reduced cell number. H_2O_2 (1 mmol/L), was used as positive control for necrotic-cell death). Results presented as mean ± SEM; $p \leq 0.05$: *; $p \leq 0.01$: **; $p \leq 0.001$: ***; $p \leq 0.0001$: ****. N = 3-4.

activation.

2.3. Experimental design

aHSCs were treated with different concentrations of doxazosin (Sigma-Aldrich, USA) (from 2.5 μmol/L to 50 μmol/L). Based on the dose-effect studies, 10 μmol/L was used for all experiments (Fig. 1). Cells were exposed to TGF-β (2.5 ng/mL) to obtain maximal activation. NE at 10 μmol/L (Sigma-Aldrich, USA) was used as an agonist for α1-AR, phorbol 12-myristate 13 acetate (PMA) as an activator of PKC at 100 nmol/L and m-3M3FBS as an activator of PLC at 25 μmol/L (Sigma-Aldrich, Amsterdam, The Netherlands). qHSCs were treated with TGF-β (2.5 ng/mL) as a positive control of activation and doxazosin 10 μmol/L as indicated. Each experiment was repeated at least 3 times, using cells from different isolations.

2.4. Sytox Green cell toxicity determination

Toxicity was determined using Sytox Green nucleic acid staining (Invitrogen, The Netherlands), diluted 1:40000 in culture medium and applied at the end of treatments for 15 min at 37 °C. Fluorescent detection was performed with a Leica fluorescence microscope using an excitation wavelength of 450−490 nm. H_2O_2 (1 mmol/L) was used as a positive control for necrosis.

2.5. Colorimetric MTT (tetrazolium) viability assay

aHSCs were seeded in 96-well plates (5000 cells/well) and treated as indicated. After 72 h, cell viability was analyzed using MTT assay as described (Mosmann, 1983). Colorimetry was analyzed by iMark™Microplate absorbance reader from BioRad Laboratories (wavelength of 595 nm and a reference wavelength of 655 nm).

2.6. Isolation of mRNA, cDNA synthesis and RT-PCR

mRNA was isolated from cells using TRIzol® reagent according to supplier's instructions (Thermo Fisher Scientific). Total mRNA was quantified with a Nanodrop 2000c UV–vis spectrophotometer (Thermo Fisher Scientific) and stored at −80°C until use. Reverse transcription was performed on 2.5 μg of total RNA using random nonamers and M-MLV reverse transcriptase (Invitrogen, USA). Subsequently, real-time quantitative PCR was performed using the qPCR core kit master mix (Eurogentec, The Netherlands) on a 7900 H T Fast Real Time PCR System (Applied Biosystems, Foster City, CA, USA). Relative expression levels were normalized to 36b4 as an internal housekeeping gene and presented as relative levels compared to the control condition set to 1. PCR primers are listed in Table 1.

2.7. Western blot analysis

At the end of the experiments, cells were scraped, and lysates were prepared by 4 cycles of freezing (-80 °C) and thawing (37 °C) followed by centrifugation for 15 min at 12,000 rpm to obtain protein lysates. Protein concentration was quantified by Bio-Rad protein assay (Bio-Rad, Hercules, CA, USA). Western blot (WB) analysis was performed as described (Damba et al., 2019). Primary antibodies are listed in Table 2. Images were captured with Chemidoc MR (Bio-Rad) system. The intensity of bands was quantified with ImageJ version 2.0.0-rc-69/1.52n.

2.8. Cell proliferation assay

aHSC proliferation was measured by BrdU assay and Real-Time xCELLigence system. The BrdU assay was performed according to the manufacturer's instruction. For Real-Time xCELLigence system (RTCA DP; ACEA Biosciences, Inc., CA, USA), cells were seeded in a 16-well E-plate and treated as indicated. Cell index was determined by the xCELLigence system.

2.9. Senescence-associated β-galactosidase staining

SA-β-Gal staining was determined by Senescence-associated β-galactosidase staining kit (Cell Signaling Technology, Danvers, Massachusetts, USA) using manufacturer's protocol. Images were captured by digital phase contrast microscopy.

2.10. Immunofluorescence Microscopy (IF)

aHSCs were seeded in 12-well plates containing 18 mm glass coverslips (CS) and treated with TGF-β (2.5 ng/mL) and/or DX10 μmol/L. After 72 h of exposure, cells on coverslips were washed, fixed (4% PFA, 10 min) and permeabilized (0.1 % Triton X-100, 10 min), prior to non-specific blocking (2% BSA, 30 min). After blocking, cells on coverslips were incubated 1 h at RT in presence of primary antibody goat polyclonal collagen type 1 (Southern Biotech, 1310-01) and mouse monoclonal αSMA (Sigma Aldrich, A5228) (See Table 2), after first antibody, cells were washed 3 times and then incubated with secondary antibodies goat anti-rabbit Alexa Flour 488 or rabbit anti-mouse Alexa Flour 488 (Thermo Fisher Scientific) for 30 min at RT. Finally, cells in CS, were washed three times and mounted with Vectashield Antifade Mounting Medium with DAPI (Vector Laboratories, Gdynia, Poland). CS were air-dried, sealed using nail polish and store at 4 °C, covered from light until further use. Images were taken with Leica Fluorescence microscope (Leica Microsystems, Wetzlar, Germany) and processed using ImageJ software version 2.0.0-rc-69/1.52n.

Table 2
WB and immunofluorescence antibodies.

Protein	Species	Dilution	Company
Collagen Type 1	Polyclonal-goat	WB 1:2000, IF 1:500	1310-01, Southern Biotech
αSMA	Monoclonal-mouse	WB 1:2000, IF 1:500	A5228, Sigma Aldrich
P21 (Gene is *Cdkn1a*)	Monoclonal-rabbit	1:1000	ab109199, Abcam
GAPDH	Monoclonal-mouse	1:1000	CB1001, Calbiochem
p-PKC	Polyclonal rabbit	WB 1:2000	ab59411, Abcam

Table 1
Sequences of PCR primers.

Gene	Forward 5′–3′	Reverse 5′–3′	Probe 5′–3′
36b4	GCTTCATTGTGGGAGCAGACA	CATGGTGTTCTTGCCCATCAG	TCCAAGCAGATGCAGCAGATCCGC
Col1α1	TGGTGAACGTGGTGTACAAGGT	CAGTATCACCCTTGGCACCAT	TCCTGCTGGTCCCCGAGGAAACA
Acta2 (αSMA)	GCCAGTCGCCATCAGGAAC	CACACCAGAGCTGTGCTGTCTT	CTTCACACATAGCTGGAGCAGCTTCTCGA
Ppar γ	CAC AAT GCC ATC AGG TTT GG	GCT GGT CGA TAT CAC TGG AGA TC	CCA ACA GCT TCT CCT TCT CGG CCT G
Tp53 (p53)	CCATGAGCGTTGCTCTGATG	CAGATACTCAGCATACGGATTTCCT	CGGCCTGGCTCCTCCCCAAC
Cdkn1a (p21)	TTGTCGCTGTCTTGCACTCTG	CGCTTGGAGTGATAGAAATCTGTTA	CTGCCTCCGTTTTCGGCCCTG
Il-6	CCGGAGAGGAGACTTCACAGA	AGAATTGCCATTGCACAACTCTT	ACCACTTCACAAGTCGGAGGCTTAATTACA
Mmp9	CCCTCTGCATGAAGACGACAT	GGAGGTGCAGTGGGACACA	TCCAGCATCTGTATGGTCGTGGCTCTAAAC

2.11. Statistical analysis

GraphPad Prism 7.0 was used for statistical analysis. Data are presented as mean ± standard error of the mean (SEM) of each group. All experiments were repeated at least 3 times. Statistical significance between mean values were assessed using the two-way ANOVA and t-tests, as appropriate. P-values ≤0.05 were considered significant.

3. Results

3.1. Determination of doxazosin treatment concentration

Fully activated primary HSCs (aHSCs) were treated with different concentrations of DX. As shown in Fig. 1, DX at concentrations from 2.5 to 20 μmol/L was not toxic to aHSCs, whereas 50 μmol/L was clearly toxic. In addition, MTT assay showed no toxic effects of doxazosin between 2.5−20 μmol/L (Fig. 1B). Based on the toxicity studies, we used 10 μmol/L of DX in all subsequent experiments.

3.2. Doxazosin reduces fibrotic markers, but not Acta2 expression in aHSC

To determine whether doxazosin has an effect on the fibrogenic phenotype of aHSCs, gene expression of *Acta2*, *Col1α1* and *Mmp9*, as well as the protein expression of collagen type 1 and αSMA were analyzed. DX did not modify the expression of *Acta2* at mRNA and protein levels (Fig. 2A), indicating that DX does not affect the expression of this cytoskeletal protein which is involved in the contractile function of aHSCs. In contrast, *Col1α1* gene expression was significantly downregulated by DX compared to non-treated cells (Fig. 2B). On the other hand, DX is not as efficient in lowering *Col1α1* expression in TGF-β-treated aHSCs. Although a tendency to decrease the expression of *Col1α1* is observed this did not reach statistical significance (Fig. 2B). In contrast, DX significantly reduced collagen type 1 at the protein level in TGF-β-treated aHSCs, indicating that TGF-β was not able to restore collagen type 1 protein level in the presence of DX (Fig. 2B). A similar pattern was observed by immunofluorescence staining for collagen type 1: total collagen type 1 (permeabilized cells) and secreted collagen type 1 (non-permeabilized cells) were both decreased in DX-treated aHSCs (Fig. 2C). The anti-fibrotic action of DX on aHSCs was also observed in the presence of TGF-β (Fig. 2B-C). To confirm the antifibrotic effect of DX observed with collagen type 1, we analyzed the mRNA expression of *Mmp9*. DX significantly upregulates *Mmp9* expression compared to non-treated cells. In addition, DX restored *Mmp9* expression in the presence of TGF-β (Fig. 2D). In order to determine whether DX was able to stop or delay the activation of HSCs, mRNA expression of *Acta2*, *Col1α1* and *Pparγ* were analyzed in quiescent stellate cells. For *Acta2* and *Col1α1*, DX significantly decreased their mRNA levels in comparison to non-treated cells. Moreover, DX maintained the downregulation of the expression of *Col1α1* in the presence of TGF-β. In line with this, the expression of the

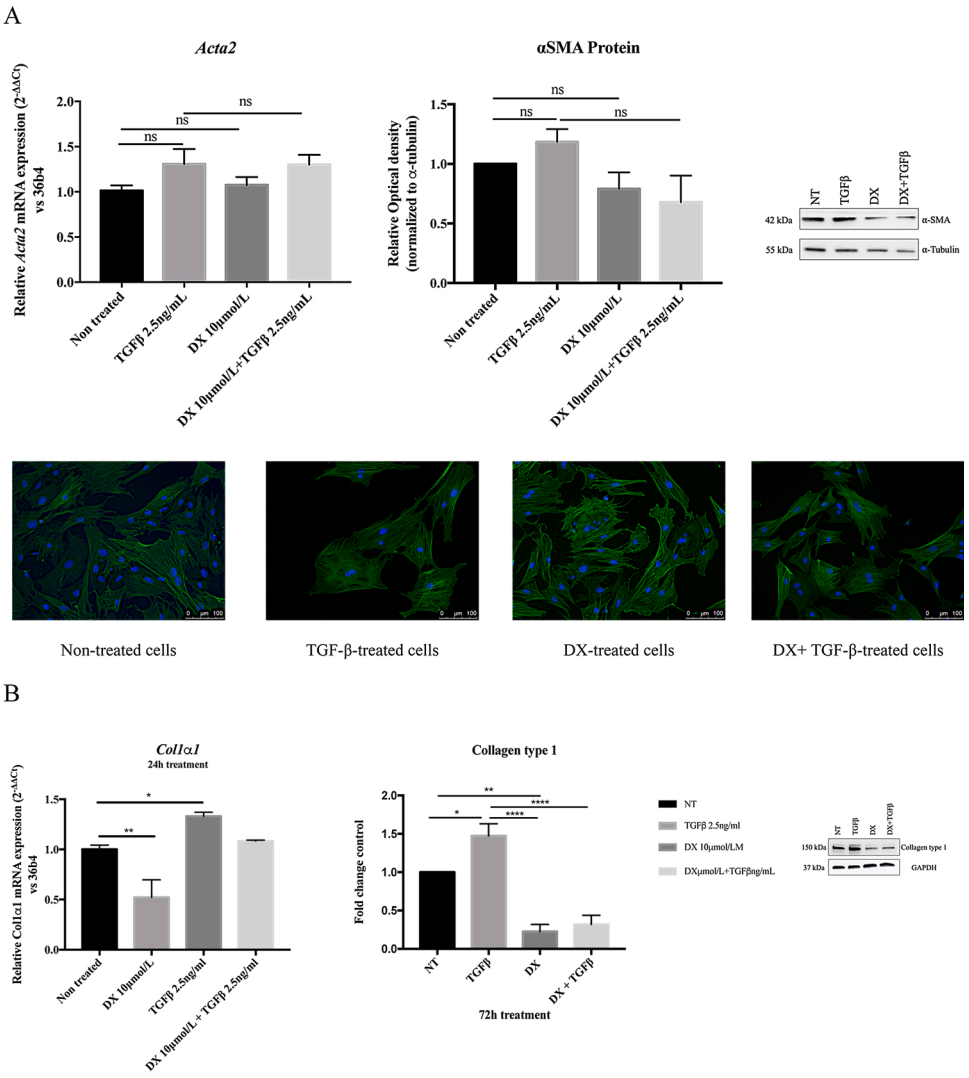

Fig. 2. Fibrogenic markers in aHSCs are decreased by DX. A: Expression of αSMA at mRNA and protein level, measured after 72 h of exposure with DX and/or TGF-β. **B:** collagen type 1 at mRNA and protein level in aHSCs measured after 24 h or 72 h treatment with DX and/or TGF-β, respetively. GAPDH and α tubulin were used as loading control for protein detection and 36b4 as housekeeping gene. **C:** Representative images of collagen type 1 immunofluorescence (green) and DAPI (blue) after 72 h treatment with DX and/or TGF-β; scale bar 50 μm. **D:** Relative gene expression of *Mmp9* after 72 h treatment with DX and/or TGF-β (36b4 as housekeeping gene). **E:** mRNA expression of *Acta2*, *Col1α1* and *Pparγ* in quiescent HSCs after 72 h treatment with DX and/or TGF-β (36b4 as housekeeping gene). Results are presented as mean ± SEM; $p \leq 0.05$: *; $p \leq 0.01$: **; $p \leq 0.001$: ***; $p \leq 0.0001$: ****. n = 3-4.

C

Permeabilized

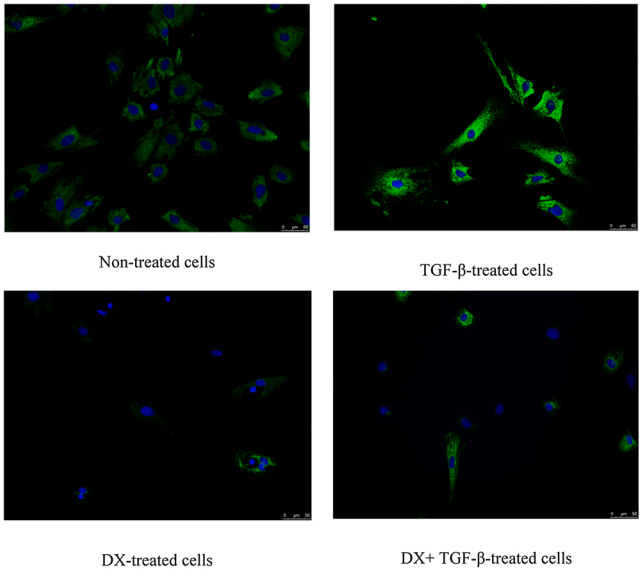

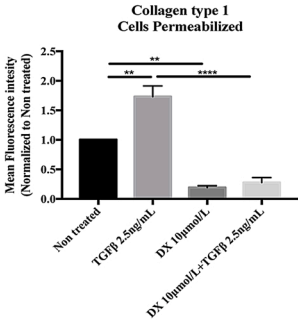

Non-Permeabilized

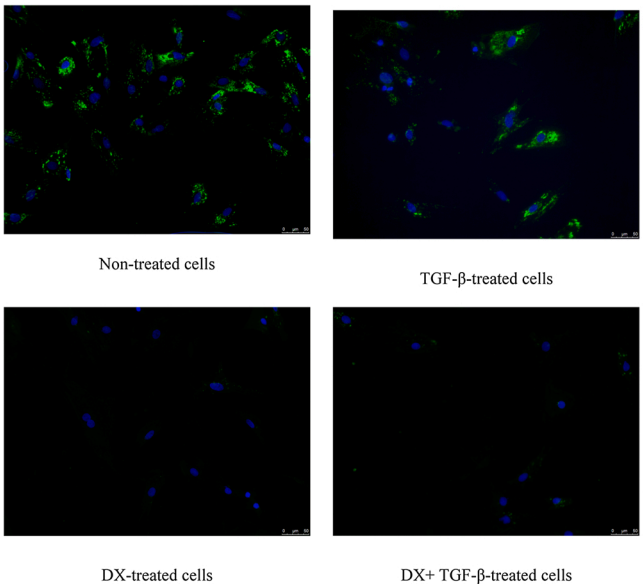

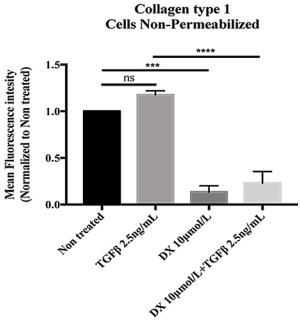

Fig. 2. (*continued*).

quiescence marker *Pparγ* was increased by DX in both control and TGF-β-treated cells with statistical significance, demonstrating that DX delays hepatic stellate cells activation in addition to the antifibrotic properties observed in aHSCs.

3.3. Doxazosin reduces proliferation of aHSCs

Next, the effect of DX on proliferation of aHSCs was assessed. Cultured aHSCs were seeded with or without DX for 72 h. Doxazosin significantly reduced cell proliferation (Fig. 3A-B).

3.4. Doxazosin induces the expression of senescence markers in aHSC

In order to determine whether the antiproliferative effect of DX was linked to cellular senescence in aHSCs, senescence and quiescence markers were analyzed. aHSCs were treated for 72 h with or without DX. A significant increase in *Cdkn1a* (p21) and *Tp53* was observed (Fig. 4A). p21 protein expression was also determined after of DX-treatment by WB exhibiting the same pattern as observed at the mRNA level (Fig. 4B). DX-treatment also increased the number of β-galactosidase positive cells (Fig. 4C). mRNA expression of *Pparγ* was analyzed by qPCR. This marker is highly expressed in quiescent HSCs but is also involved in progression of senescence. Our results showed a significant increase in the expression of *Pparγ* in DX-treated cells (Fig. 4A).

3.5. Doxazosin increases mRNA levels of SASP in aHSCs

In order to determine whether DX induces SASP in aHSCs we tested *IL-6*, *IL-1β*, *Mmp9*, *Mmp2* and *Timp1* since their expression is high in senescent cells. As shown in Fig. 5, DX markedly induced the mRNA expression of SASP markers.

Fig. 2. (*continued*).

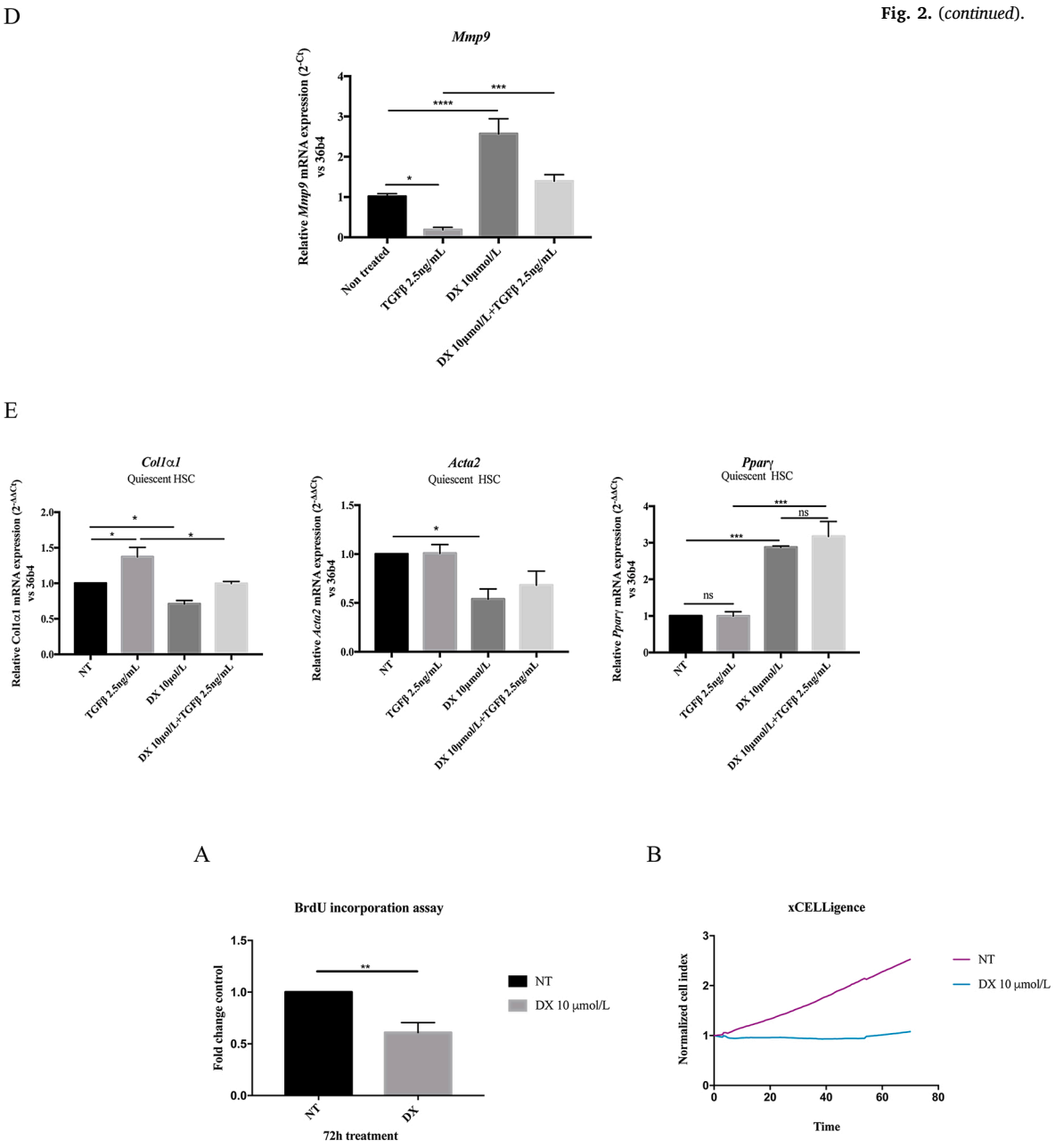

Fig. 3. Doxazosin treatment decreases cell proliferation of aHSCs. Cell proliferation was measured by the BrdU incorporation assay (**A**) and xCelligence real time (**B**). Cell proliferation is represented by cell index. Results are represented as mean ± SEM; p ≤ 0.01: **. n = 3-4.

3.6. Doxazosin induces senescence via alpha-1 AR antagonism

Next, we investigated whether the induction of senescence by doxazosin was dependent on antagonism of the alpha-1 AR. NE was used as a non-selective agonist of the alpha-1 AR on aHSCs. NE alone did not change cell proliferation (Fig. 6A). In addition, NE did not have any effect on both *cdkn1a* and *Tp53*. In contrast, DX inhibited cell proliferation in the absence and presence of NE (Fig. 6A) and DX significantly increased *cdkn1a* and *Tp53* expression, also in the presence of NE (Fig. 6B). We next addressed the potential mechanisms for the observed effects of DX and NE by investigating the role of the alpha-1 AR downstream signaling intermediates PKC and PLC. We used PMA as PKC activator and m-3M3FBS as PLC activator. Both activators alone tended to increase aHSCs proliferation, but a statistically significant increase was only achieved by PMA. Both activators appeared to reverse the effect of DX on cell proliferation, but these effects did not reach statistical significance compared to the non-treated group (Fig. 6C). Both activators had no effect on the expression of senescence markers at the mRNA level (Fig. 6D) and they did not abolish the pro-senescence effects of DX on *cdkn1a* and *Tp53* expression. In contrast, both activators did reverse the DX-induced increase of p21 protein expression (Fig. 6E). In addition, the activators of PKC and PLC reversed the increase of β-galactosidase positive cells induced by DX (Fig. 6F). These results indicate that the pro-senescence effect of DX is dependent on alpha-1 antagonism and can be (partly) reversed by activating downstream PKC and PLC signaling. To reinforce these results, we analyzed the activation of PKC by WB. DX decreased p-PKC expression but this did not reach statistical significance compared to non-treated cells. However, both PMA and m-3M3FBS increased phospo-PKC levels compared to non-treated cells. This result indicates that phosphorylation of PKC is increased by both PMA and m-3M3FBS and reduced by DX (Fig. 6G). Next, we tested the role of PKC and PLC in regulating the expression of collagen type 1 at mRNA and

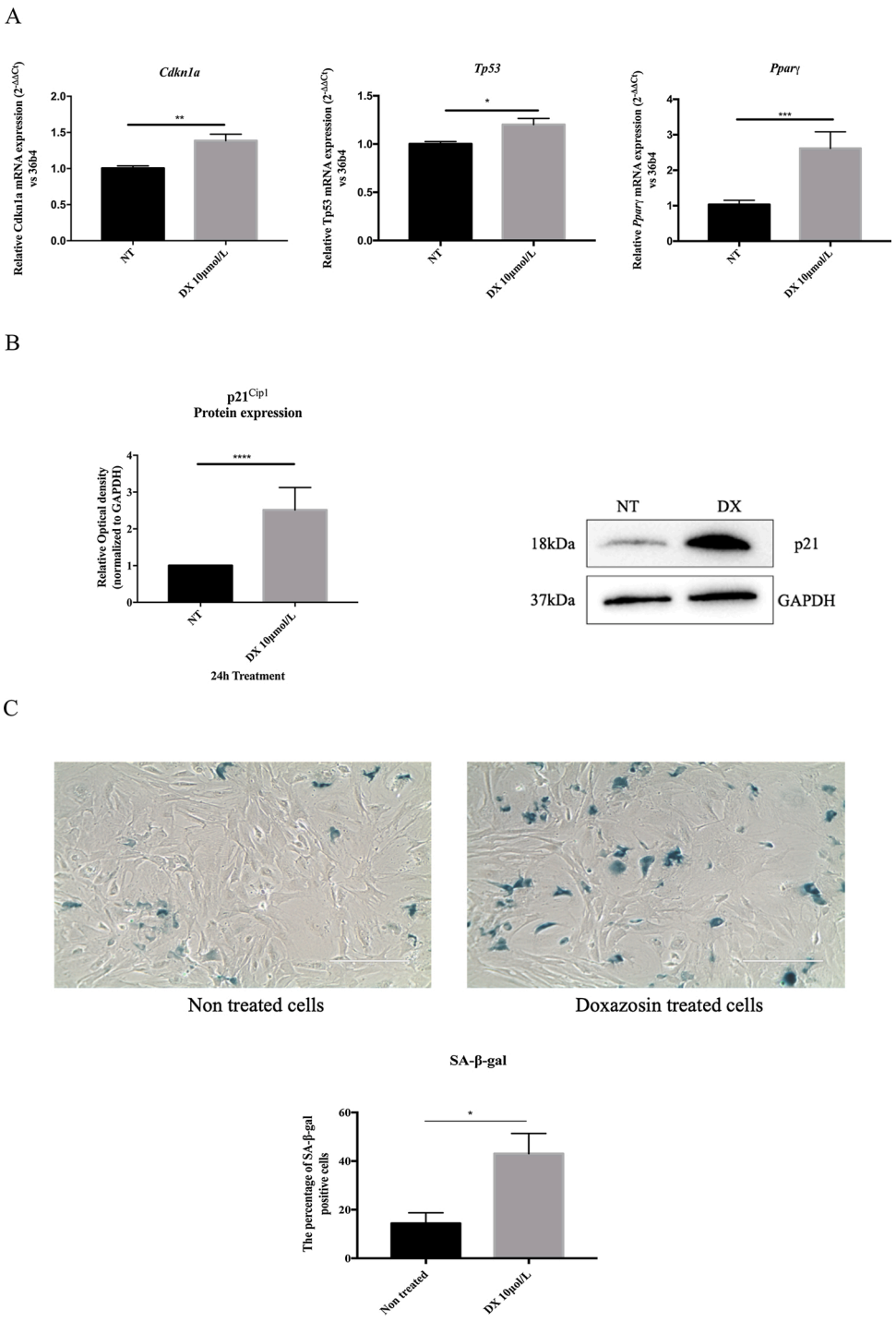

Fig. 4. Doxazosin induces cellular senescence. A: mRNA expression of *Cdkn1α* and *p53* after 72 h treatment with DX. 36b4 (housekeeping gene). **B:** increased $P21^{Cip1}$ protein expression after 24 h treatment with DX. GAPDH (loading control). **C:** SA-β-gal staining. Scale bar: 200 μm (magnification 10X) after 72 h treatment with DX. Results are presented as mean ± SEM; $p \leq 0.05$: *. n = 3-4.

protein level by using PMA and m-3M3FBS, in order to find a relationship between alpha-1 AR signaling and fibrogenic activity, considering that the senescent phenotype decreases the fibrogenic activity of aHSCs. As expected, DX downregulated the expression of collagen type 1 significantly. In contrast, PMA (200 nmol/L) and m-3M3FBS (25 μmol/L), had no effect on collagen type 1 expression, both at the mRNA and protein level and completely abolished the antifibrotic effect of DX (Fig. 6H).

4. Discussion

Previously, we demonstrated that the α1-AR antagonist doxazosin decreases collagen deposition in liver tissue *in vivo* (Serna-Salas et al., 2018), however, the exact anti-fibrotic mechanism of doxazosin has not been elucidated yet. Anti-inflammatory effects of doxazosin were reported in rodent models of inflammation (Tung et al., 2013). It is possible that the anti-fibrotic effect of doxazosin is indirect *via* reducing liver inflammation. In this study, we show that doxazosin also targets aHSCs, by decreasing expression of collagen type 1 at protein and mRNA

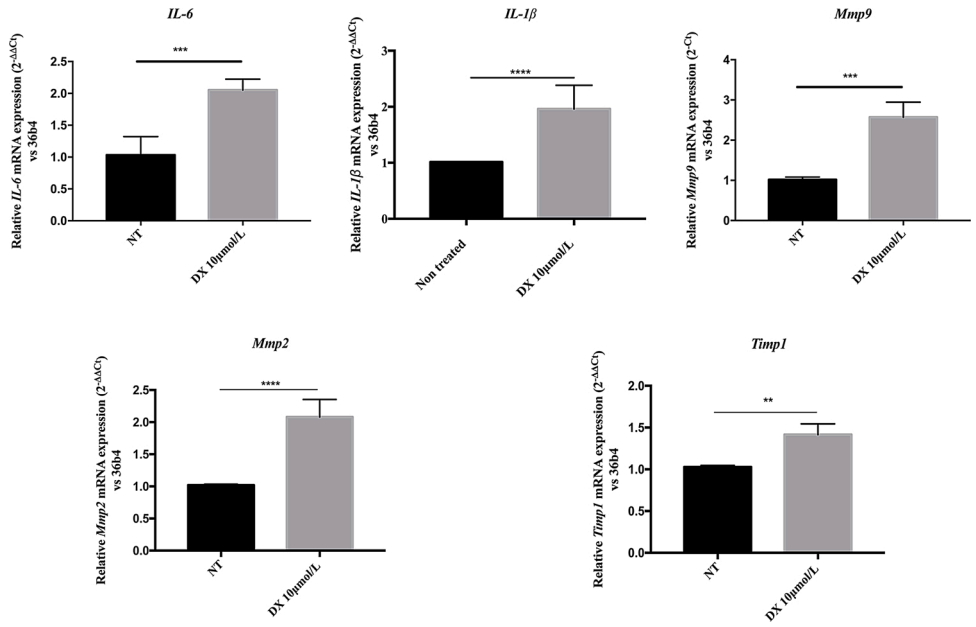

Fig. 5. Doxazosin increases expression of SASP markers. mRNA expression of *IL-6*, *IL-1β Mmp9, Mmp2 and Timp1* is increased in aHSCs after 72 h treatment with DX. Results are presented as mean ± SEM; $p \leq 0.05$: *; $p \leq 0.01$: **; $p \leq 0.001$: ***. n = 3-4.

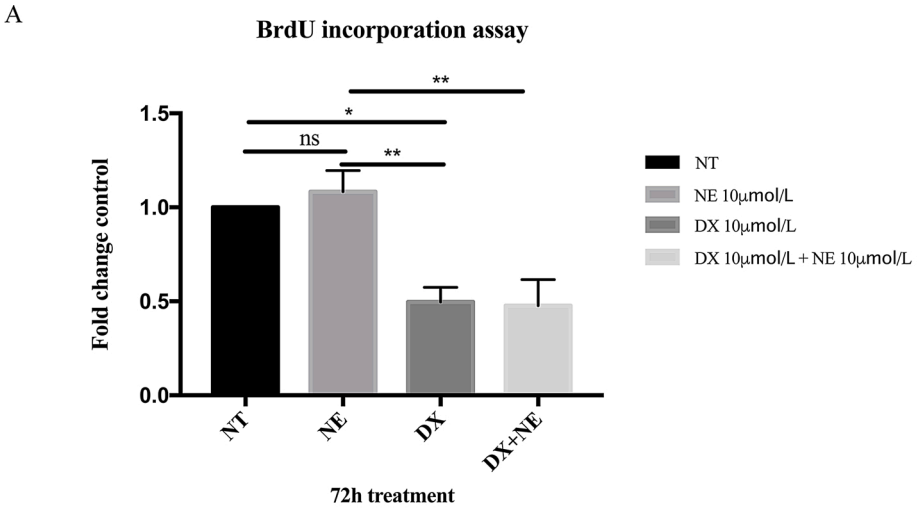

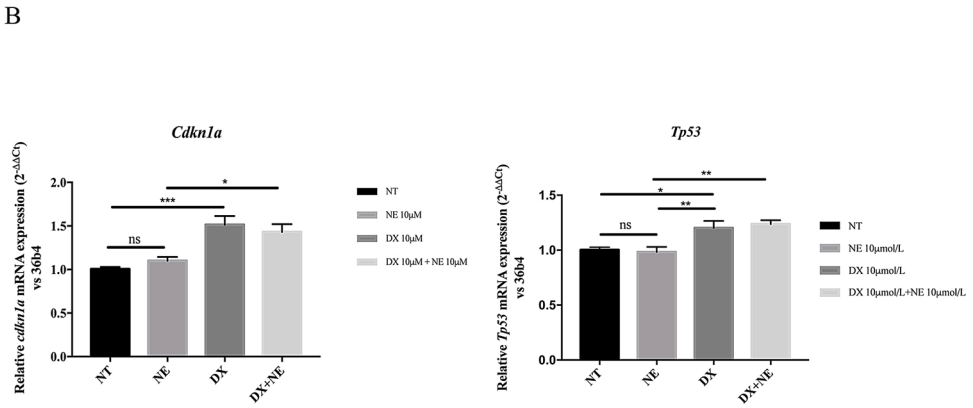

Fig. 6. Doxazosin induces cellular senescence *via* alpha-1 antagonism. aHSCs were cultured with DX with or without NE, PMA or m-3M3FBS. **A:** cell proliferation by BrdU incorporation assay was evaluated after 72 h, no effect observed with NE. **B**: *cdkn1a* and *Tp53* gene expression were analyzed after 72 h (NE treatment). **C-D:** PKC activation increased cell proliferation but had no effect on *cdkn1a* and *Tp53* (data analyzed after 72 h treatment). PLC activation did not affect cell proliferation nor the expression of senescence markers. **E**: $P21^{Cip1}$ protein expression was not affected by PMA or m-3M3FBS alone. DX increased $P21^{Cip1}$ protein expression and this increase was abolished by PMA and m-3M3FBS. GAPDH: loading control (protein expression was analyzed after 24 h treatment). **F**: SA-β-gal activity of aHSCs was increased after 72 h treatment with DX. This increase was reversed by PMA and m-3M3FBS (magnification 10X). **G**: p-PKC protein level was decreased by DX. Decreased p-PKC protein expression by DX was abolished by PMA and m-3M3FBS. GAPDH: loading control, (protein expression was analyzed after 24 h treatment). **H:** Collagen type 1 expression was decreased by DX at both mRNA and Protein level. Decreased Collagen type 1 by DX was abolished by PMA and m-3M3FBS. GAPDH: loading control, and 36b4 housekeeping gene (data analyzed after 72 h treatment). Results are presented as mean ± SEM; $p \leq 0.05$: *. n = 3-4.

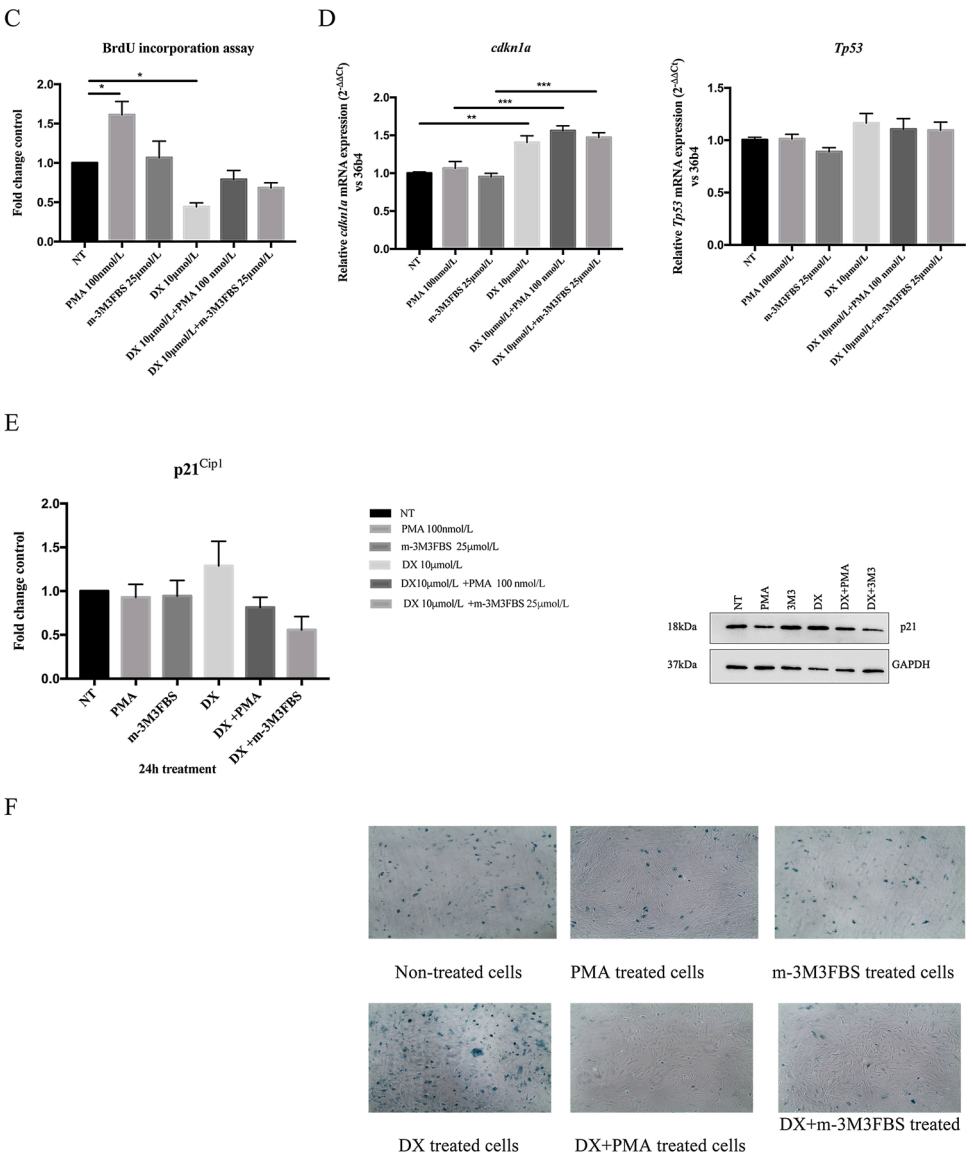

Fig. 6. (*continued*).

level. However, the mRNA expression of αSMA was not changed by doxazosin. DX did increase *Mmp*9 expression. This metalloproteinase is known to be downregulated in activated hepatic stellate cells. Moreover, in an animal model of cirrhosis, increased expression of MMP9 correlated with a decrease in the index of fibrosis (Hernández-Ortega et al., 2012; Lachowski et al., 2019; Qin and Han, 2010). These results suggest that doxazosin only affects the fibrogenic properties of these cells but not their morphology and/or contractility. In addition, other experiments were performed in quiescent hepatic stellate cells, to determine whether DX was able to stop or slow down HSCs activation. DX downregulates Col1α1 and ACTA2 and increased the expression of the quiescence marker PPARγ, both in the presence and absence of TGF-β, confirming that DX delays stellate cell activation.

Proliferation is one of the most important characteristics of activated hepatic stellate cells (Kocabayoglu et al., 2015). In our studies, we demonstrated that doxazosin also has an anti-proliferative effect on aHSCs.

Cellular senescence is a process that limits cell growth since it induces a permanent state of cell cycle arrest (Petrova et al., 2016; Zhang et al., 2021). It has been reported that senescence of aHSC decreases the accumulation of ECM and facilitates the resolution of fibrosis, whereas senescent aHSCs maintain their expression of αSMA, GFAP and vimentin (Krizhanovsky et al., 2008). Additional studies have reported that αSMA is still present in senescent cells (Mellone et al., 2017; Meyer et al., 2016). Considering that DX diminished collagen type 1 expression and proliferation without an effect on αSMA expression, we speculated that the anti-fibrotic and anti-proliferative effects of doxazosin on aHSCs are linked to senescence. Cellular senescence is mediated by the p53/p21 and p16/Rb pathways (Krizhanovsky et al., 2008), which arrests the cell cycle at the G1 phase (Al-Haj et al., 2012). Increased expression of p53 and p21, but not p16, was observed in senescent aHSCs (Chen et al., 2016) suggesting that senescence pathways may be cell type specific. In addition, in a model of liver fibrosis, increased deposition of fibrotic tissue was observed in $p53^{-/-}$ mice compared to wild-type mice, accompanied by a decreased SA-β-gal staining in stellate cells of $p53^{-/-}$ mice (Krizhanovsky et al., 2008)). Our results demonstrate that doxazosin limits the proliferation of aHSCs by inducing senescence, since doxazosin treatment increases the expression of senescence markers. Furthermore, senescent cells present a SASP characterized by increased expression of IL-6 which has been associated with DNA damage (Coppé et al., 2008). In addition to IL-6, which is an accepted marker and prominent cytokine of the SASP, IL-1β is also produced and secreted by senescent cells (Coppé et al., 2010a,b), as well as several proteases like MMP2 and MMP9 (Aoshiba et al., 2013). In our study, we also observed

Fig. 6. (*continued*).

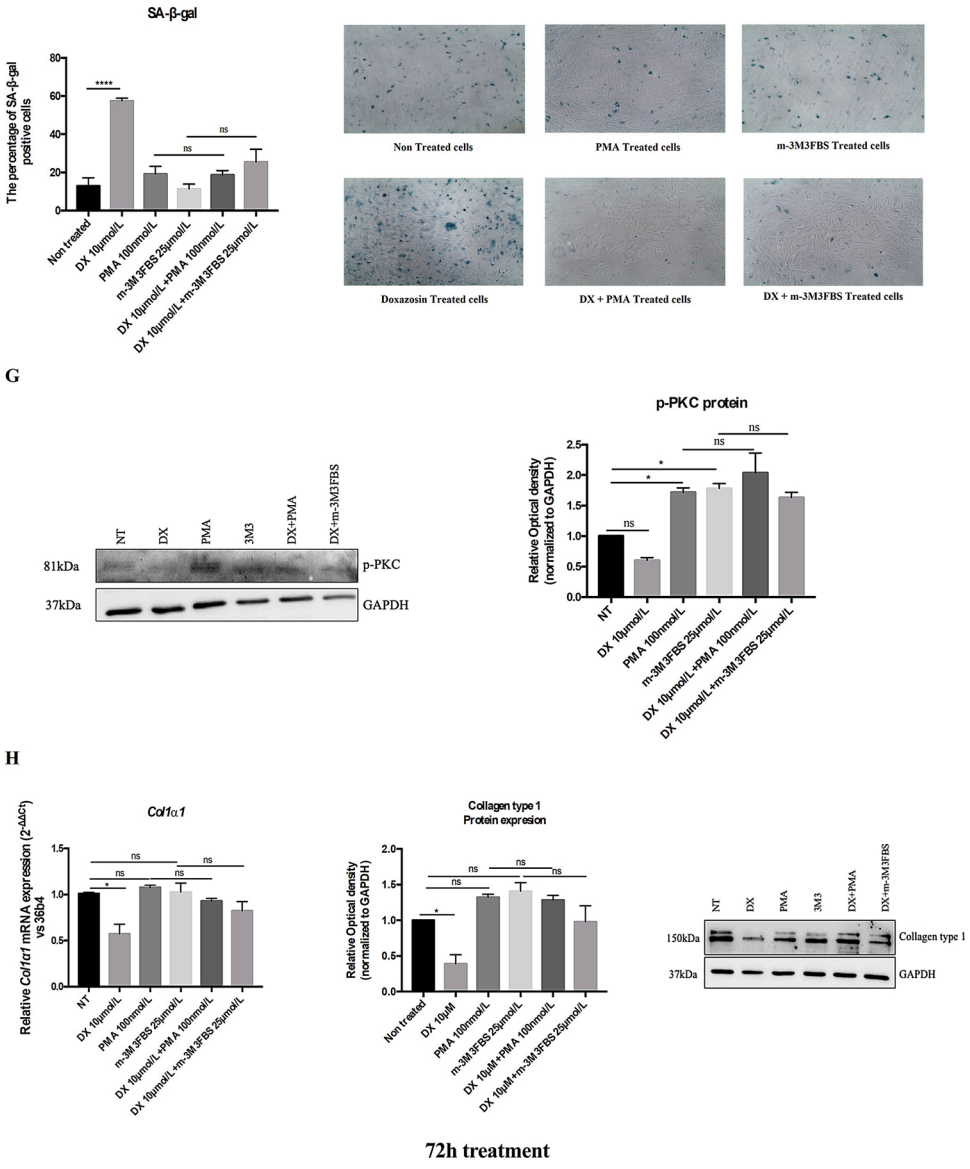

increased expression of IL-6, IL-1β, MMP2, MMP9 and TIMP1 in aHSCs treated with doxazosin. An interesting observation in our study is the increased expression of PPARγ mRNA following doxazosin treatment. PPARγ is a ligand dependent transcription factor, important in vitamin A metabolism in HSCs (Tardelli et al., 2017). Its expression and activity are high in quiescent HSCs but suppressed in aHSCs (Hazra et al., 2004). Previous studies demonstrated that the induction of PPARγ expression inhibits proliferation of aHSCs (Xu et al., 2003). Whether the increased expression of PPARγ is cause or consequence of the induction of senescence remains to be elucidated. Agonists of PPARγ have anti-proliferative effects on aHSCs by reducing the number of cells in the S phase of the cell cycle (Marra et al., 2000) and this effect appears to be related to increased p53 expression and induction of senescence of aHSCs (Jin et al., 2016). Together, these studies and our results suggest that increasing the expression of PPARγ in aHSCs may induce a senescent phenotype rather than a quiescent phenotype and may play an important role in the resolution of fibrosis. In addition, we observed that doxazosin induced the activity of SA-β-gal. However, although SA-β-gal has been used as a senescence biomarker, it is not highly specific (Lee et al., 2006), therefore its detection cannot be used as the only marker to define the senescent state.

Since our results demonstrate the induction of senescence in aHSCs by doxazosin, we investigated the possible signaling pathways involved. Previous studies reported that norepinephrine is able to increase HSCs proliferation and its effect is mediated *via* the α1-AR (Oben et al., 2003). Based on those reports and the anti-proliferative response upon antagonism of α1-AR on aHSCs, we hypothesized that the α1-AR antagonist could contribute to the induction of senescence. We used norepinephrine as an agonist of α1-AR. Contrary to what was observed in previous studies by Oben et al. (2003), NE did not influence the proliferation of aHSCs, whereas doxazosin significantly decreased the proliferation of aHSCs in both the presence and absence of NE. Besides the inhibition of proliferation of aHSCs, doxazosin also increased expression of *cdkn1a* and *Tp53* even in presence of NE. According to these results, we assumed that doxazosin induces senescence independent of its α-1AR antagonism, however, to further clarify this mechanism and because norepinephrine is not a selective α-1AR agonist, we used activators of downstream signaling intermediates of α-1AR signaling. It has been described that PKC activation increases cell growth rates in rat hepatic stellate cells (Ramm et al., 2003). Moreover, downregulation of PKC activity has been

associated with senescence in human diploid IMR-90 fibroblasts (Park et al., 2017). Finally, a study by Govekar et al. (2012) showed that inhibition of PKC activity induces a senescent phenotype in human erythrocytes. As expected, PMA increased aHSC proliferation. Interestingly, PMA also restored the reduced proliferation in the presence of doxazosin. The same pattern was observed with m-3M3FBS. Furthermore, the expression of p21 and β-galactosidase activity were also inhibited by the use of PMA or m-3M3FBS in presence of doxazosin. As described before, it appears that PKC activity is related to the induction of senescence and the senescence phenotype abolishes the fibrotic activity of aHSCs (Krizhanovsky et al., 2008; Chen et al., 2016). Our results support the notion that senescence markers are regulated by the PKC and PLC pathways. We show in this study that both PMA and m-3M3FBS increase the phosphorylation of PKC. DX reduced the phosphorylation of PKC demonstrating that alpha-1 adrenergic signaling is blocked by DX and reversed by PMA and m-3M3FBS. Moreover, we observed a correlation between phosphorylation of PKC and the fibrogenic activity of aHSC and that the expression of collagen type 1 was restored by treatment with either PMA or m-3M3FBS in the presence of DX. All our results support the hypothesis that the effects of doxazosin on senescence induction in aHSCs is dependent on α-1 AR antagonism and that the effects of doxazosin can be reversed by PKC and/or PLC agonists.

In conclusion, the results of this study demonstrated that doxazosin reduces the fibrogenic activity of aHSCs which is linked with the induction of cellular senescence *via* α1 AR antagonism, suggesting that α1-AR is a novel therapeutic target to treat liver fibrosis. On the other hand, although senescence induction is a promising therapeutic strategy to reverse hepatic fibrogenesis, the existence of a sustained SASP can have negative consequences for tissues and organs since the pro-inflammatory profile of senescent cells can lead to enhanced proliferation and tumorigenesis of epithelial cells (Laberge et al., 2012). The cytokines released as part of the SASP have effects on natural killer cells (NK cells) and may contribute to the clearance of senescent (tumor) cells (Di Mitri and Alimonti, 2016). It is necessary to continue research on the possible application of senescence induction for the treatment of liver fibrosis, taking into account the potential long-term side effects of senescence.

Author contributions

Concept and design: S.A. Serna-Salas, M.H. Muñoz-Ortega, J. Ventura-Juarez, H. Moshage; methodology: S.A. Serna-Salas, M. Zhang, T. Damba; acquisition of data: S.A. Serna-Salas; analysis and interpretation of data: S.A. Serna-Salas, M. Zhang, T. Damba, H. Moshage; resources: H. Moshage, J. Ventura-Juarez, M.H. Muñoz-Ortega; technical assistance: M. Buist-Homan; writing-original draft preparation: S.A. Serna-Salas, J.C. Arroyave-Ospina; writing review: M.H. Muñoz-Ortega, J. Ventura-Juarez, H. Moshage: study supervision - M.H. Muñoz-Ortega, J. Ventura-Juarez, H. Moshage.

Funding

Project no. A1-S-21375, CONACyT, Mexico, Fellowship no. 701914 CONACyT to Sandra Alejandra Serna Salas.

Availability of data and materials

The data used to support the findings of this study are available from the corresponding author upon request.

Ethics approval and consent to participate

All animal care complied with the legal requirements approved by the guidelines of Institutional Animal Care and Use Committee of Laboratory Animals of the University of Groningen (DEC-RUG). Experimental procedures were approved by the appropriate Animal ethics Committee.

Consent for publication

Not applicable.

Declaration of Competing Interest

The authors declare that they have no competing interest.

Data availability

No data was used for the research described in the article.

Acknowledgements

This study was supported by CONACyT Funds, Project no. A1-S-21375. Mexico.

References

Al-Haj, L., Blackshear, P.J., Khabar, K., 2012. Regulation of p21/CIP1/WAF-1 mediated cell-cycle arrest by RNase L and tristetraprolin, and involvement of AU-rich elements. Nucleic Acids Res. 40 (16), 7739–7752.
Aoshiba, K., et al., 2013. Senescence-associated secretory phenotype in a mouse model of bleomycin-induced lung injury. Exp. Toxicol. Pathol. 65, 1053–1062.
Chen, J., et al., 2016. Soluble egg antigens of Schistosoma japonicum induce senescence in activated hepatic stellate cells by activation of the STAT3/p53/p21 pathway. Sci. Rep. 6, 1–11.
Coppé, J., et al., 2008. Senescence-associated secretory phenotypes reveal cell-nonautonomous functions of oncogenic RAS and the p53 tumor suppressor. PLoS Biol. 6 (12), e301.
Coppé, J., Desprez, P., Krtolica, A., Campisi, J., 2010a. The Senescence-Associated Secretory: the dark side of tumor suppression. Annu. Rev. Pathol. 5, 99–118.
Coppé, J., et al., 2010b. The Senescence-Asociated Secretory: the dark side of tumor supression. Annu. Rev. Pathol. Mech. Dis. 99–118.
Damba, T., et al., 2019. Hydrogen sulfide stimulates activation of hepatic stellate cells through increased cellular bio-energetics. Nitric Oxide 92, 26–33.
Di Mitri, D., Alimonti, A., 2016. Non-cell-autonomous regulation of cellular senescence in cancer. Trends Cell Biol. 26 (3), 215–226.
Dimri, G.P., et al., 1995. A biomarker that identifies senescent human cells in culture and in aging skin in vivo. Proc. Natl. Acad. Sci. 92, 9363–9367.
García-Sáinz, J.A., Vázquez-Prado, J., Villalobos-Molina, R., 1999. α1-Adrenoceptors: subtypes, signaling, and roles in health and disease. Arch. Med. Res. 30 (6), 449–458.
Govekar, R.B., et al., 2012. Reduced PKC α activity induces senecent phenotype in erythrocytes. Anemia. P8139:1-7.
Han, C., Bowen, W.C., Michalopoulos, G.K., Wu, T., 2008. Alpha-1 adrenergic receptor transactivates signal transducer and activator of transcription-3 (Stat3) through activation of Src and epidermal growth factor receptor (EGFR) in hepatocytes. J. Cell. Physiol. 216 (2), 486–497.
Hazra, S., et al., 2004. Peroxisome proliferator-activated receptor γ induces a phenotypic switch from activated to quiescent hepatic stellate cells. J. Biol. Chem. 279 (12), 11392–11401.
Hernández-Ortega, L.D., et al., 2012. Quercetin improves hepatic fibrosis reducing hepatic stellate cells and regulating pro-fibrogenic/anti-fibrogenic molecules balance. J. Gastroenterol. Hepatol. (Australia) 27 (12), 1865–1872.
Jin, H., et al., 2016. Activation of PPARγ/p53 signaling is required for curcumin to induce hepatic stellate cell senescence. Cell Death Dis. 7, e2189.
Kocabayoglu, P., et al., 2015. β-PDGF receptor expressed by hepatic stellate cells regulates fibrosis in murine liver injury, but not carcinogenesis. J. Hepatol. 63 (1), 141–147.
Krizhanovsky, V., et al., 2008. Senescence of activated stellate cells limits liver fibrosis. Chem. Eng. News 134 (4), 657–667.
Laberge, R.M., Awad, P., Campisi, J., Desprez, P.Y., 2012. Epithelial-mesenchymal transition induced by senescent fibroblasts. Cancer Microenviron. 5 (1), 39–44.
Lachowski, D., et al., 2019. Matrix stiffness modulates the activity of MMP-9 and TIMP-1 in hepatic stellate cells to perpetuate fibrosis. Sci. Rep. 9 (1), 1–9.
Lee, B., et al., 2006. Senescence-associated β-galactosidase is lysosomal β-galactosidase. Aging Cell 5, 187–195.
Marra, F., et al., 2000. Ligands of peroxisome proliferator-activated receptor γ modulate profibrogenic and proinflammatory actions in hepatic stellate cells. Gastroenterology 119 (2), 466–478.
Mellone, M., et al., 2017. Induction of fibroblast senescence generates a non-fibrogenic myofibroblast phenotype that differentially impacts on cancer prognosis. Aging 9 (11), 114–132.
Meyer, K., et al., 2016. Essential Role for premature senescence of myfibroblasts in myocardial fibrosis. J. Am. Coll. Cardiol. 67 (17), 2018–2028.

Mosmann, T., 1983. Rapid colorimetric assay for cellular growth and survival: application to proliferation and cytotoxicity assays. J. Immunol. Methods 65 (1–2), 55–63.
Narita, M., et al., 2003. Rb-mediated heterochromatin formation and silencing of E2F target genes during cellular senescence. Cell 113 (6), 703–716.
Oben, J.A., et al., 2003. Norepinephrine and neuropeptide Y promote proliferation and collagen gene expression of hepatic myofibroblastic stellate cells. Biochem. Biophys. Res. Commun. 302 (4), 685–690.
Park, J.W., Lee, Y.H., Bae, Y.S., 2017. Protein kinase C downregulation induces senescence via FoxO3a inhibition in HCT116 and HEK293 cells. Biochem. Biophys. Res. Commun. 493 (4), 1548–1554.
Petrova, N.V., Velichko, A.K., Razin, S.V., Kantidze, O.L., 2016. Small molecule compounds that induce cellular senescence. Aging Cell 15 (6), 999–1017.
Qin, L., Han, Y.P., 2010. Epigenetic repression of matrix metalloproteinases in myofibroblastic hepatic stellate cells through histone deacetylases 4: implication in tissue fibrosis. Am. J. Pathol. 177 (4), 1915–1928.
Ramm, G.A., Li, L., Britton, R.S., O'Neill, R., Bacon, B.R., 2003. Effect of protein kinase C activation and inhibition on rat hepatic stellate cell activation. Dig. Dis. Sci. 48 (4), 790–796.
Rippe, R.A., Brenner, D.A., 2004. From quiescence to activation: gene regulation in hepatic stellate cells. Gastroenterology 127 (4), 1260–1262.
Schnabl, B., Purbeck, C.A., Choi, Y.H., Hagedorn, C.H., Brenner, D.A., 2003. Replicative senescence of activated human hepatic stellate cells is accompanied by a pronounced inflammatory but less fibrogenic phenotype. Hepatology 37 (3), 653–664.
Serna-Salas, S.A., et al., 2018. Doxazosin and carvedilol treatment improves hepatic regeneration in a Hamster model of cirrhosis. BioMed Res. Int. https://doi.org/10.1155/2018/4706976, 4706976.
Sigala, B., et al., 2013. Sympathetic nervous system catecholamines and neuropeptide Y neurotransmitters are upregulated in human NAFLD and modulate the fibrogenic function of hepatic stellate cells. PLoS One 8 (9), 1–13.
Strosberg, A.D., 1993. Structure, function, and regulation of adrenergic receptors. Protein Sci. 2 (8), 1198–1209.
Tardelli, M., et al., 2017. AQP3 is regulated by PPARγ and JNK in hepatic stellate cells carrying PNPLA3 I148M. Sci. Rep. 7 (1), 1–10.
Tung, D., Ciallella, J., Cheung, P.H., Saha, S., 2013. Novel anti-inflammatory effects of doxazosin in rodent models of inflammation. Pharmacology 91, 29–34.
Xu, J., Fu, Y., Chen, A., 2003. Activation of peroxisome proliferator-activated receptor-γ contributes to the inhibitory effects of curcumin on rat hepatic stellate cell growth. Am. J. Physiol. Gastrointest. Liver Physiol. 285, G20–G30.
Zhang, M., et al., 2021. Hepatic stellate cell senescence in liver fibrosis: characteristics, mechanisms and perspectives. Mech. Ageing Dev. 199.